

Photophysics of 7-Azaindole, Its Doubly-H-Bonded Base-Pair, and Corresponding Proton-Transfer-Tautomer Dimeric Species, via Defining Experimental and Theoretical Results

Javier Catalán[†] and Michael Kasha^{*‡}

Departamento de Química Física Aplicada, Universidad Autónoma de Madrid, Cantoblanco, E-28049 Madrid, Spain, and Institute of Molecular Biophysics and Department of Chemistry, Florida State University, Tallahassee, Florida 32306-4380

Received: August 4, 2000; In Final Form: September 13, 2000

Photophysical research on the experimental and theoretical bases for the biprotonic transfer in the doubly-H-bonded dimer of 7-azaindole (7AI) is reported. The spectroscopic properties of the 7AI monomer, the normal-tautomer dimer, and the proton-transfer tautomer dimer are delineated by absorption, fluorescence and excitation spectra. The monomeric 7AI molecule is shown to exist at 10^{-6} M in hydrocarbon solution at 298 K, and the pure dimer at temperatures below 227 K in 10^{-4} M solution in 2-methylbutane (2MB). Deuteration of the pyrrolic sites yields dimers which exhibit only normal-tautomer fluorescence, whereas the nondeuterated 7AI dimer yields unique proton-transfer tautomer fluorescence, indicating quantum-mechanical tunneling as the principal mechanism for the biprotonic transfer. Density functional theory (B3LYP/6-31G** framework) calculations on the ground-state potential energy curves conform to the experimental results.

Introduction

In the Watson–Crick model for DNA,¹ the genetic code is related to the situation of the protons that yield the linkage of base pairs via hydrogen bonds. Such a code can be altered either spontaneously or via external perturbations.^{2,3} The molecular basis of mutations related to alteration of the DNA code has been the focus of extensive studies since the Watson and Crick suggestion¹ of anomalous pairing via formation of tautomers of some bases. Hydrogen-bond tunneling,⁴ isomerization of bases,⁵ pyrimidine dimers,⁶ effect of ionizing radiation and UV irradiation,^{3,6–12} formation of eximers^{13–15} have all been addressed as contributing to mutations.

The discovery of double-proton-transfer¹⁶ in an electronically excited model base pair, 7AI dimer (Scheme 1), has promoted extensive experimental and theoretical study of the 7AI doubly-H-bonded dimer since 1969. These studies have revealed unexpected complexity, even in the excitation mechanism for this simple base pair.^{17–20}

From evidence derived by picosecond laser spectroscopy, Eisenthal et al.²¹ found double proton transfer in 7AI dimer to occur in less than 5 ps at both 298 and 77 K, and photo-tautomerization at 77 K to be wavelength dependent. On the basis of mass-selected multiphoton ionization (MPI) and laser-induced-fluorescence (LIF)—supersonic-jet molecular beam studies, Fuke et al.^{22,23} confirmed the tautomerization in the lowest excited state ($S_1^n(D)$) of the dimer. Bulska et al.^{24,25} suggested that, the proton transfer in the dimer could result via tunneling immediately after excitation, and at least a hundred times more slowly by crossing over the potential barrier. They also concluded that F_1 was from normal tautomer dimer species and also from 7AI H-bonded chain oligomers. Itoh et al.²⁶ found the dual fluorescence of the normal-tautomer dimer and its proton-transfer tautomer (PT-tautomer) to exhibit a pronounced isotopic effect over the temperature range 130–200 K.

In rigid-glass solutions of 7AI in 3MP at 77 K, Kasha et al.¹⁶ detected a structured phosphorescence emission with its onset at 430 nm; their 77 K luminescence spectrum for 7AI at 10^{-5} M in 3MP (hydrocarbon) solvent appears to be for 7AI monomer, probably as a result of the quick-freezing technique (their Figure 3). An analogous phosphorescence observed at 77 K in ethanol glass solution was assigned to the normal-tautomer 7AI monomer. In 1980, Bulska and Chodkowska²⁰ measured the phosphorescence (in 3MP at 77). A comparison of their 7AI dimer phosphorescence spectrum at 77 K in 3MP and the onset of the fluorescence spectrum obtained by El-Bayoumi et al.^{17,18} revealed that both were strikingly similar in energetic and vibronic terms, confirming the observation of El-Bayoumi et al. Measurements showed that, at low temperature, the PT-tautomer fluorescence was overlapped by the isoenergetic phosphorescence of the normal-tautomer monomer. Bulska and Chodkowska²⁰ also found the green fluorescence in 3MP to be unstructured above 115 K, and vibronic structure and long-lived emission to occur only below 110 K. In 1981, Waluk, Bulska et al.²⁴ found the phosphorescence spectrum to be almost isoenergetic with F_2 . Accordingly, Bulska et al.²⁴ concluded that the phosphorescing triplets are generated via PT-tautomer singlets and that the origin of the phosphorescence is the back proton transfer ($S_1^l(D) \rightarrow T_1^n(D) \rightarrow S_0^n(D)$). In 1984, Bulska et al.²⁵ concluded that the phosphorescence resulted from oligomers; however, they also conceded that noncyclic dimers might be the origin.

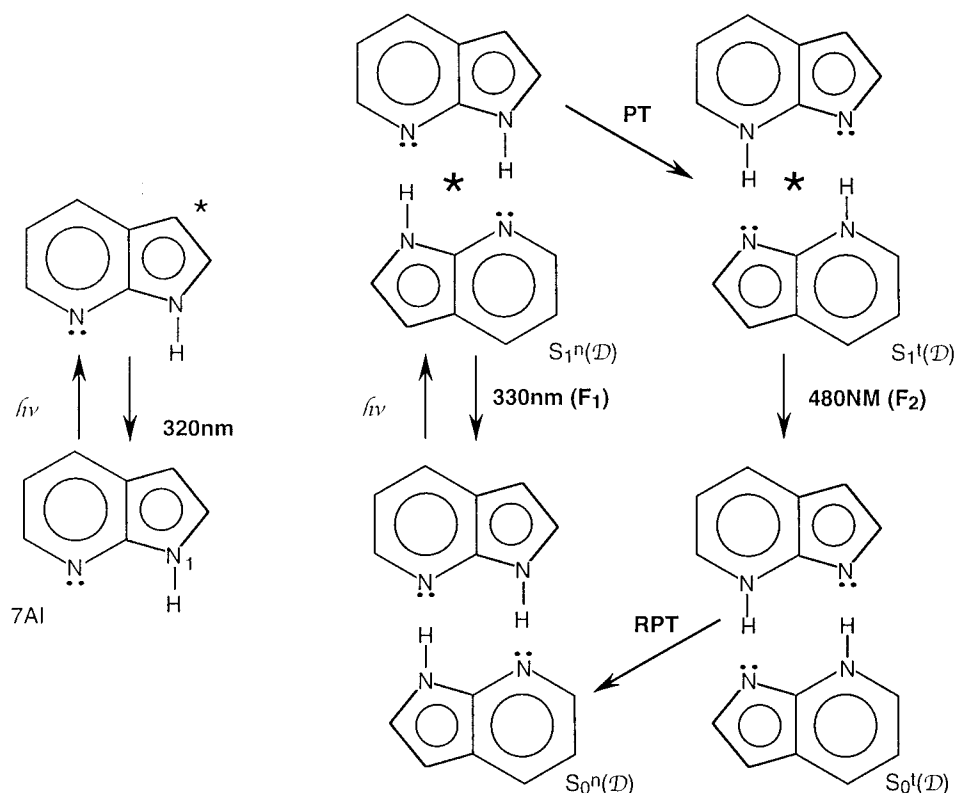
Regarding stabilization of the 7AI tautomer dimer, Kasha et al.¹⁶ found that no permanent change in 7AI dimer absorption occurred upon prolonged illumination; therefore, the quasi-stable ground-state PT-tautomer did not accumulate. There is extensive research on this point, and considerable variation in observation and interpretation.^{17,18,26–28}

Itoh et al. found the PT-tautomer in its ground electronic state to have a lifetime of 19.0 μ s at 298 K and of 183 μ s at 172 K.²⁸ In 1991, Hochstrasser et al.,²⁹ using femtosecond spec-

[†] Universidad Autónoma de Madrid.

[‡] Florida State University.

SCHEME 1



troscopy, identified a radiationless channel leading directly to the ground-state dimeric PT-tautomer from the first singlet excited-state normal-tautomer dimer. In 1997, Suzuki et al.,³⁰ using the time-resolved thermal lensing (TRTL) technique, found the PT-tautomer to be only 0.97 kcal/mol higher in energy than the normal-tautomer dimer form. Chou et al.³¹ made the more realistic (cf. ref 44) interpretation of this small value as being actually the van der Waals lowering of the dimer ground-state $S_0^n(D)$ energy below that of the monomer ground-state $S_0^n(M)$ (both for the normal tautomer, vide infra). In 1998, Zewail et al.³² found no evidence of PT-tautomer absorption ($S_0^t \rightarrow S_1^t$), consistent with the results of earlier experiments at 77 K.¹⁷ Paradoxically, Chou et al.³¹ in 1998 asserted that the PT-tautomer species could be trapped in the ground electronic state, and analyzed its kinetic, photochemical, and spectroscopic behavior.

The controversy over the photophysical properties of such an interesting chromophore as 7AI dimer is probably the result of using samples with high optical densities, and the high risk of generating optical artifacts involved. Such an essential tool for the photophysicist as the excitation spectrum has been reported in only a few of the reported papers; also, some of the spectra published are rather inadequate (for example, see Figure 3 in refs 25 and 27).

This paper reports the results of comprehensive experimental work on various photophysical properties of 7AI dimer in the condensed phase, with special emphasis on the identification of the excited species in each instance on the basis of the corresponding excitation spectrum.

This work was undertaken with aim of answering the following questions:

- Does 7AI dimer (normal tautomer) exhibit dual fluorescence?
- Does the double-proton-transfer in 7AI dimer take place by thermal activation or by tunneling?

- Are the 7AI normal-tautomer ($T_1^n(D)$) and PT-tautomer ($T_1^t(D)$) triplet states of 7AI observable as phosphorescence?

- Can the dimeric PT-tautomer ($S_0^t(D)$) be trapped in its ground electronic state for a measurable period of time?

Experimental and Theoretical Section

7-Azaindole was obtained from Sigma in 99% purity and recrystallized twice in spectroscopic-grade cyclohexane. All 7AI solutions in 2-methylbutane (Aldrich, anhydrous form). The cryostat was purged with dried Nitrogen 99.99% purity. N_1 -deuterated 7-azaindole was prepared by refluxing 7-azaindole in alkaline D_2O for 1 h. NMR revealed an isotopic purity of at least 90%.

Unless otherwise stated, all 7AI solutions were 10^{-4} M. All spectroscopic measurements in Suprasil quartz cylindrical cells of 3 mm optical path; consequently, the light path to the cell center, which governs the so-called "filtering effect" on fluorescence (a major factor with highly absorbing solutions), was less than 1.5 mm—the average path length ranging from 0 to 1.5 mm. The sample temperature, which was varied over the range 293–77 K, was controlled by an Oxford DN1704 cryostat equipped with ITC4 controller, interfaced to the spectrophotometers. UV–visible spectra were recorded by a Cary-5 spectrophotometer.

Corrected fluorescence and excitation spectra were obtained by using a precalibrated Aminco-Bowman AB2 spectrofluorometer. 7AI samples were excited at 315 ± 4 nm by using light from a continuous (CW) 150 W xenon lamp for steady-state spectra. Phosphorescence spectra were excited by a 7 W pulsed xenon lamp.

Computational methods based on density functional theory (DFT) applied to molecular properties have grown dramatically in recent years. All DFT computations reported in this paper were carried out by the Gaussian 94 software suite,³³ using the 6-31G** basis set.³⁴

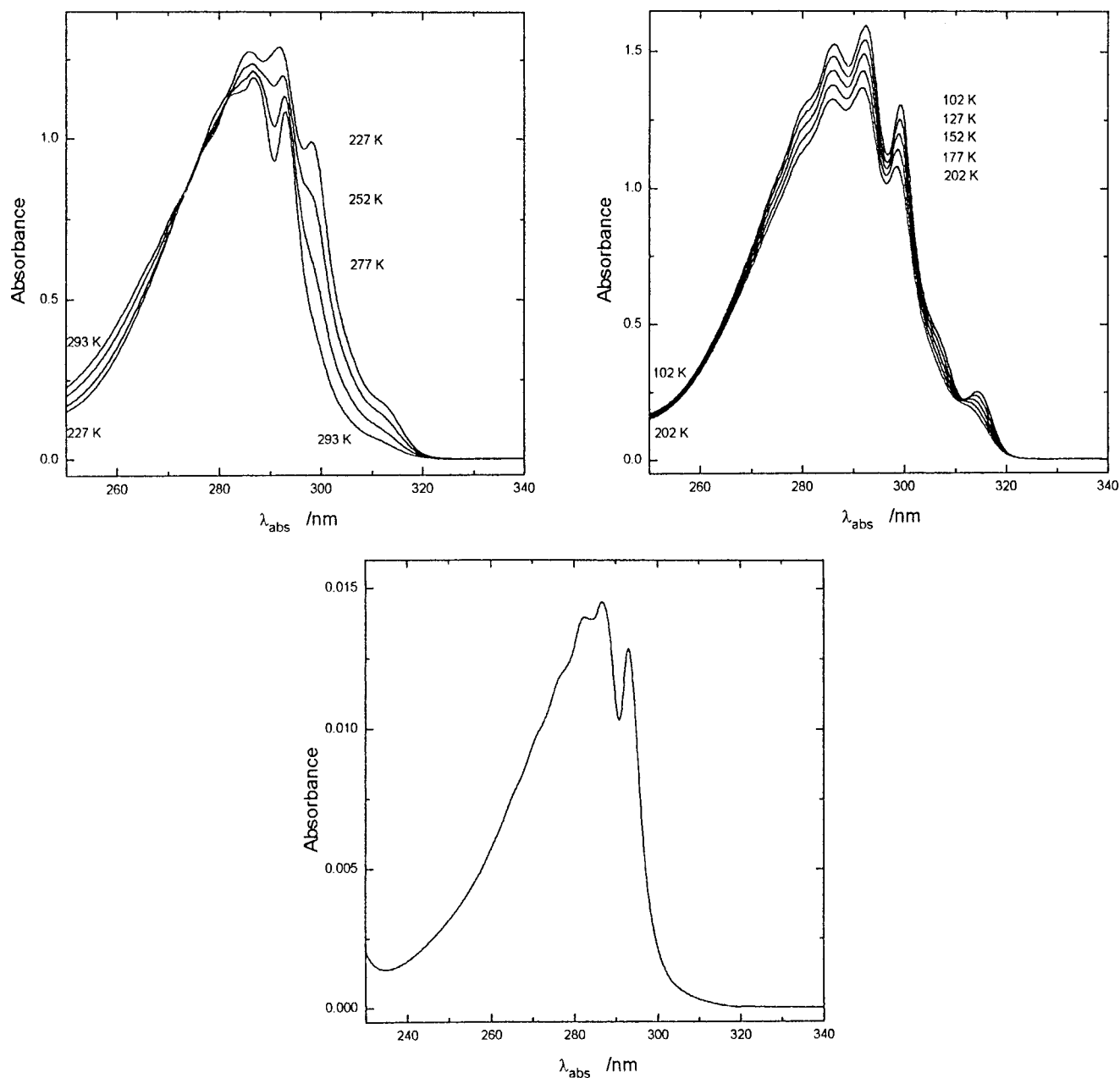


Figure 1. (1A, left) Near-ultraviolet absorption spectra for 10^{-4} M solution of 7-azaindole in 2MB at 293, 277, 252, 227 K. (B, right) Near-ultraviolet absorption spectra for 10^{-4} M solution of 7-azaindole in 2MB at 202–102 K. (C, center) Near-ultraviolet absorption spectra for 10^{-6} M solution of 7-azaindole in 2MB at 293 K.

DFT computations were done by using a hybrid functional corresponding to Becke's three-parameter exchange functional (B3LYP)³⁵ as implemented in Gaussian 94. As shown later on, this computational procedure can accurately predict the potential energy curve for the ground electronic state of a compound that describes a proton transfer via an intramolecular hydrogen bond.^{36,37}

Results and Discussion

In their 1969 paper, Kasha et al.¹⁶ reported near-UV absorption spectra for 7AI in 3MP at 293 and 77 K, both normalized at the absorption maximum (Figure 2 in ref 16); they assigned such spectra to 7AI monomer and dimer, respectively. These two spectra are so different that they raise immediate questions such as (a) is the change in the absorption spectrum for 7AI from 293 to 77 K simply the result of a bathochromic solvent shift accompanied by spectral structuring? (b) if 7AI is a

monomer–dimer mixture at room temperature and pure dimer at 77 K, under what temperature does the solution contain the pure dimer alone? (c) which molecular species is photoselected at the excitation wavelength used? Answering these questions properly entails studying the photophysics of 7AI at various temperatures in the condensed phase.

Near-UV Absorption Spectra of 7AI in 2-Methylbutane (2MB). For a given concentration of 7AI dissolved in an inert solvent such as 2MB, decreasing the solution temperature will necessarily displace the monomer/dimer equilibrium and hence lead to an absorption spectral isosbestic point. If the whole sample consists of pure dimer at a given temperature, then cooling the sample will not exhibit an isosbestic point as the curve will merely reflect cooling (and a solution absorbance increase). These two situations are clearly apparent in Figure 1A,B, which show the spectra obtained at 293, 277, 252, and 227 K, and those at 202, 177, 152, 127, and 102 K, respectively.

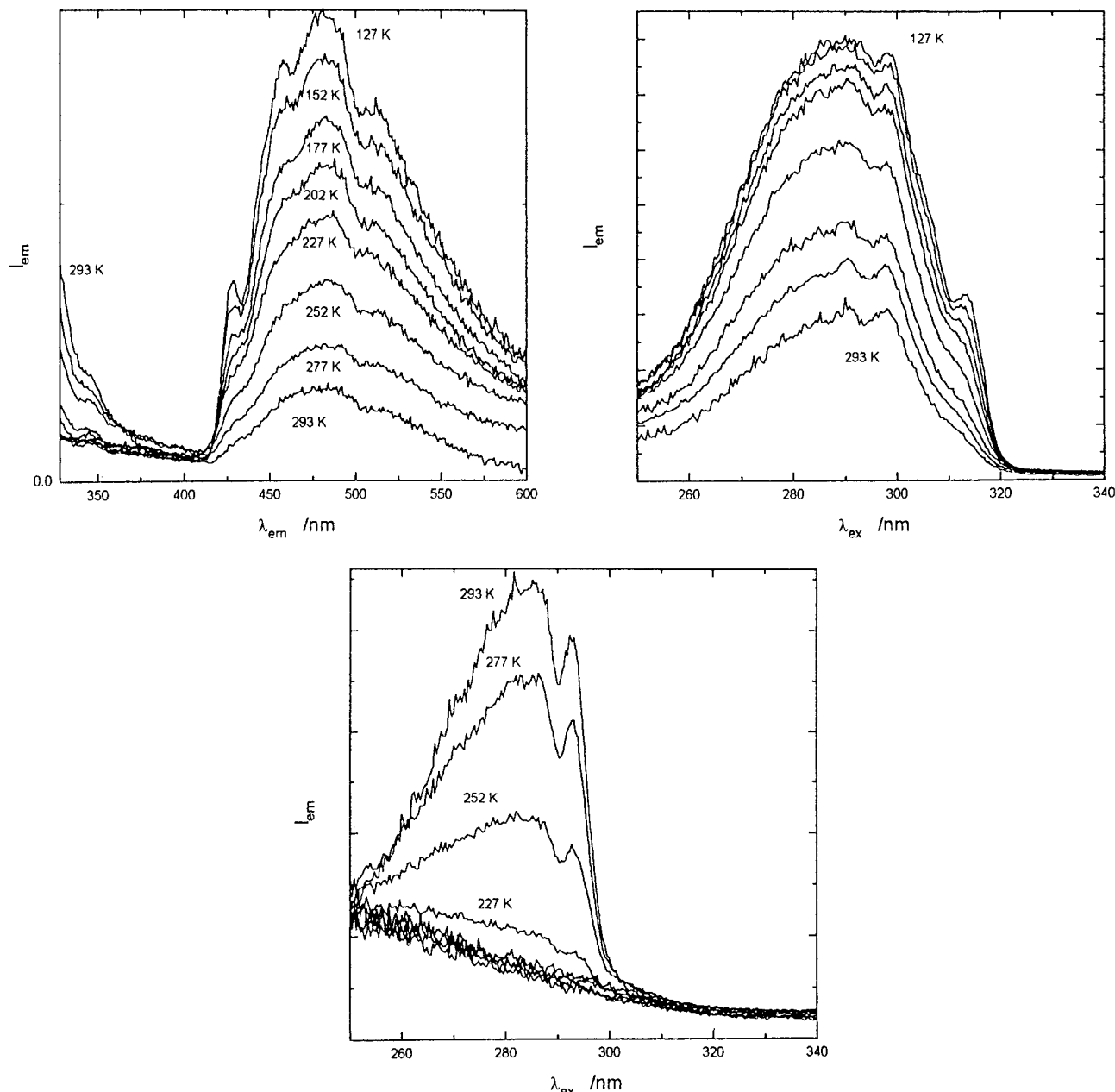


Figure 2. (2A, left) Emission spectra for 10^{-4} M solution of 7-azaindole in 2MB at 293–127 K ($\lambda_{\text{exc}} = 315$ nm). (B, right) Excitation spectra obtained monitoring the emission light at 480 nm of 10^{-4} M solution of 7-azaindole in 2MB at 293–127 K. (C, center) Excitation spectra obtained monitoring the emission light at 380 nm of 10^{-4} M solution of 7-azaindole in 2MB at 293–127 K.

Likewise, a 10^{-4} M 7AI solution in 2MB will thus be a monomer/dimer mixture above 227 K and pure dimer below it. As can be seen from Figure 1B, the observed absorption for the pure dimer sample gradually increases in intensity (the absolute integrated intensity expected to be constant) and structuring also increases, both with lowering of temperature. The spectral changes upon lowering temperature of a solution for a single component consists of several parts. Contraction of the solution volume increases the overall optical density, this leading to an illusory absorption increase. However, the inhomogeneous broadening decreases, the peak-narrowing yielding a band half-width decrease and a real increase of peak intensity. However, as Mulliken and Rieke³⁸ have shown, the integrated oscillator strength of a transition does not change with the vibrational redistribution occurring with temperature change. The spectra of Figure 1B are appropriate both to quantify 7AI emissions change with temperature, and to examine the dimer absorption. The change from 102 to 90 K is virtually

negligible, so the spectrum at 102 K can be assigned to the dimer at low temperatures. It should also be noted that the spectrum at 293 K cannot correspond to pure monomer since the 10^{-4} M solution at room temperature is a monomer–dimer mixture. In any case, the pure monomer spectrum can be obtained by using a more dilute solution of 7AI (Figure 1C). The onset of the monomer spectral absorption is at about 305 nm.

The pure dimer first vibronic peak absorption is at 315 nm (Figure 1B) (onset at 320 nm). The 10^{-4} M solution of 7AI in 2MB is composed of pure dimer except at the highest temperatures studied; therefore this is an appropriate excitation wavelength to study the photophysics of dimeric 7AI. The presence of some monomer at the highest temperatures should pose no special problem as the spectra allow its ready quantitation.

Fluorescence of 7AI Dimer. The fluorescence spectra for 7AI for a 10^{-4} M solution in 2MB from 293 to 127 K are given in Figure 2A. The characteristic emission band appears with onset at 413 nm, the intensity of which increases with decreasing

TABLE 1: Photophysical Parameters of F_2 Fluorescence of Nondeuterated 7AI Dimer and N_1 -Deuterated 7AI Dimer at the Different Experimental Temperatures Used

T (K)	$F_2^H(T)/F_2^H(293)$	τ_2^H (ns) ^a	$\phi^{\text{rel}}/\tau_2^H$	$F_2^D(T)/F_2^H(293)$	τ_2^D (ns) ^a	$\phi^{\text{rel}}/\tau_2^D$
293	1.00 (2.35) ^b	4.97	(0.53) ^c	0.55 (1.29) ^b	8.08	(0.16)
277	1.88 (2.60)	4.83	(0.54)	0.89 (1.23)	8.87	(0.14)
252	2.80 (3.08)	5.39	(0.57)	1.83 (2.01)	10.09	(0.20)
227	3.47 (3.53)	5.96	(0.59)	3.01 (3.06)	11.32	(0.27)
202	3.46	6.52	0.53	2.91	12.54	0.23
177	3.35	7.08	0.47	2.64	13.77	0.19
152	3.79	7.64	0.50	2.62	14.99	0.17
127	4.10	8.20	0.50	2.07	16.22	0.13

^a Estimated values from the linear relationship found between the lifetime measurements by Itoh et al.²⁷ and the experimental temperature for nondeuterated 7-azaindole ($\tau_H = -0.0225 (\pm 0.0008)T + 11.058 (\pm 0.130)$, with $n = 6$, $r = 0.997$, and $sd = 0.036$ ns) and for monodeuterated 7-azaindole ($\tau_D = -0.049 (\pm 0.003)T + 22.437 (\pm 0.045)$, with $n = 6$, $r = 0.993$, and $sd = 0.127$ ns). (n , points; r , regression value; sd , standard deviation). ^b Corrected values taking into account the monomer contribution; see text. ^c Estimated values considering the previous^b correction.

temperature. This band proves to be complex in composition. Figure 2B shows the corresponding excitation spectra, obtained by monitoring fluorescence at 480 nm. On the basis of the absorption spectra of Figure 1A,B, the excitation spectra represent mainly the 7AI dimer. Figure 2C shows the excitation spectra obtained by monitoring fluorescence at 380 nm; as can be inferred clearly from the excitation band contours, these spectra represent the 7AI monomer rather than the dimer (cf. Figure 1A,B). It should be noted that intensity in these excitation spectra (Figure 2C) decreases markedly as the temperature is lowered, so much so that those signals are barely visible in the spectrum recorded at 227 K. This is consistent with the conclusion derived from the absorption spectra that 7AI occurs as a monomer/dimer mixture between 293 and 227 K, and that 7AI monomer is not detected below the latter temperature.

From the spectral evidence provided by Figure 2A–C one can conclude that 7AI dimer emits fluorescence only as the PT-tautomer species ($S_1^I(D)$) generated by double proton transfer, and not in its normal-tautomer dimeric form. Any F_1 fluorescence (normal-tautomer dimer) emitted by this latter species must be so weak that it is not detectable in the excitation spectra. This conclusion is specially relevant with a view to determining the F_2/F_1 ratio, on which assignation of the double proton transfer to tunneling has very frequently relied.

The emission bands for the PT-tautomer shown in Figure 2A exhibit a salient feature that will be discussed in greater detail below but warrants an immediate comment. The spectra recorded at the three lowest temperatures (127, 152, and 177 K), which still correspond to fluid solutions of 7AI in 2MB ($mp = 114$ K), exhibit vibronic structuring, with peaks at 420, 448, and 480 nm. Also, these emission bands ostensibly increase in intensity with decreasing temperature. The increase (Figure 2A), however, should be taken cautiously as the spectra were obtained at different amounts of absorbed photons (i.e., they were not recorded on equal absorbances at 315 nm), so the effect would be largely offset if the spectra were corrected on the basis of those in Figure 1A.

Because samples were excited from the onset of the first band of absorption from the normal-tautomer dimeric species $S_0^n(D)$, the fact that its emission was not detected can be ascribed to (a) the lack of a barrier against the double proton transfer and the consequent instantaneous generation of the PT-tautomer species ($S_1^I(D)$); (b) tunneling being much faster than fluorescence de-excitation of the normal-tautomer dimer ($S_1^n(D)$); (c) the fluorescence in the normal-tautomer dimer is a forbidden transition to its ground electronic state, by the molecular exciton selection rule.¹⁶ By analyzing the effect of deuteration of the N–H group on the photophysics of 7AI we might be able to ascertain the precise origin of this lack of emission.

It is to be noted that luminescence spectra for 7AI solutions obtained by the common quick-freeze technique (a small sample tube at 298 K being plunged into a 77 K liquid N_2 bath) yields results which are quite at variance with the equilibrium cryostat-controlled spectra reported here. Obviously, the quick-freeze method yields a nonequilibrium monomer–dimer mixture, exhibiting spectral results which vitiate conclusions derived from this method on the dynamics of excitation of the dimer.

Figure 3A shows the emission spectra for the dimer formed from monodeuterated 7AI (at pyrrolic N–H) at different temperatures. At all temperatures, an unstructured emission band in the region 400–600 nm appears that is accompanied by another, prominent band at ca. 350 nm at the lowest temperatures, the intensity of this band increasing strongly with temperature lowering.

Unlike the undeuterated ($7AI$)₂ emission (Figure 2A), the intensity of the F_2 emission for the deuterated species in Figure 3A does not increase with decreasing temperature. The spectra recorded by monitoring light at 360 nm (Figure 3B, deuterated 7AI), the emission in the UV region of Figure 3A corresponds to 7AI monomer ($S_1^n \rightarrow S_0^n$) between 293 and 227 K, and to dimer below 227 K, where the emission can be assigned to F_1 ($S_1^n(D) \rightarrow S_0^n(D)$) for the normal-tautomer dimer.

As can be seen from Figure 3C, the relative intensity of these fluorescence emissions at a given temperature also varies with the extent of deuteration of the compound. Figure 3C clearly reveals the significance of tunneling in the double proton transfer; in fact, the replacement of a pyrrolic hydrogen with a deuterium atom should scarcely alter the contribution of the thermal activation mechanism to the proton-transfer process. This is also consistent with the fact that, for the undeuterated compound as well as for the deuterated one, the ratios of quantum yields divided by lifetimes of their fluorescences F_2 are independent of the experimental temperature (see Table 1), which indicates the efficiencies of the corresponding double proton transfers are also virtually independent of the experimental temperature. This can be the result of (a) the double proton-transfer being subject to no energy barrier or (b) the transfer taking place by tunneling. The presence of F_1 fluorescence in the deuterated form and its absence from the undeuterated one clearly indicate that the underlying mechanism for the double proton transfer is tunneling.

Table 1 shows the more relevant data for these fluorescence emissions in the deuterated and undeuterated compounds. The isotopic substitution has two clear-cut effects, namely: (a) the proton transfer is significantly inhibited by deuteration, as confirmed by the fact that the intensity of fluorescence F_2 in deuterated 7AI is comparatively lower at each temperature than in undeuterated 7AI; and (b) deuteration induces fluorescence

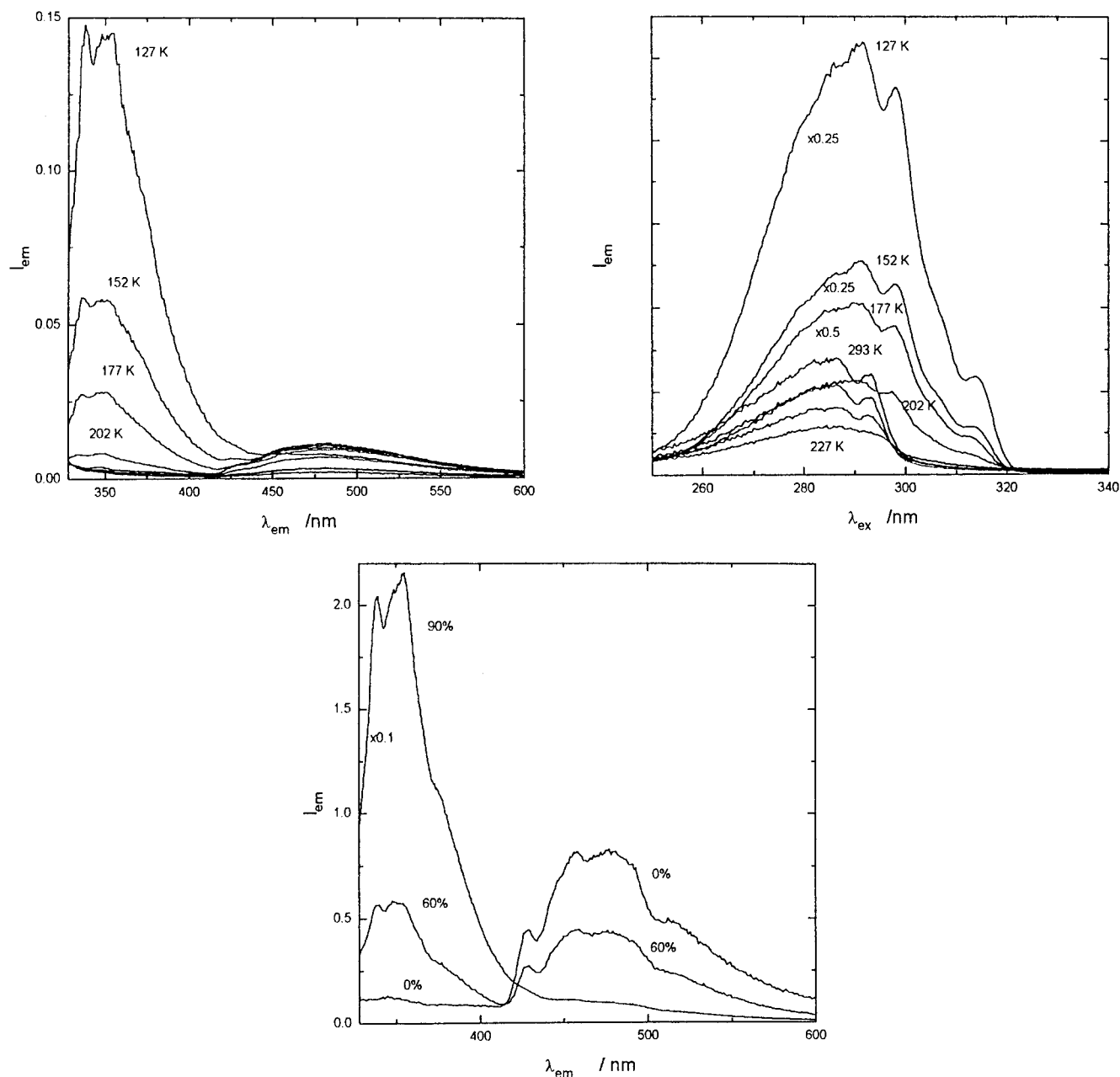


Figure 3. (3A, left) Emission spectra for 10^{-6} M solution of monodeuterated (90%) 7-azaindole in 2MB at 293–127 K ($\lambda_{exc} = 315$ nm). (B, right) Excitation spectra obtained monitoring the emission light at 360 nm of 10^{-4} M solution of monodeuterated (90%) 7-azaindole in 2MB at 293–127 K. (C, center) Emission spectra for 10^{-4} M solution of 7-azaindole in 2MB at 127 K: (a) 7-azaindole; (b) monodeuterated (60%) 7-azaindole, and (c) monodeuterated (90%) 7-azaindole ($\lambda_{exc} = 315$ nm).

F_1 in the dimeric form, which, at a low enough temperature, becomes the predominant emission.

Phosphorescence of 7AI Dimer. Figure 4A shows the luminescence spectra for 7AI and its monodeuterated derivative, both at a 10^{-4} M concentration in 2MB, obtained at 77 K with excitation at 315 nm. The spectrum for the deuterated species contains several well-defined peaks in the 420–500 nm region that traditionally have been assigned^{16,20,25} to phosphorescence emission. Note that the peaks are more ill-defined in undeuterated 7AI. The contrast of this more diffuse contour compared with the monomer phosphorescence spectrum under the same conditions (Figure 3 of ref 16) is owing to the more complex emission components exhibited by the tautomer dimer (cf. Figure 2A).

To discriminate clearly the phosphorescence from all other luminescences in the two compounds, new spectra were recorded

by using a pulsed lamp, and detecting the emission with a 300 μ s delay. As can be seen from Figure 4B, the spectrum for monodeuterated 7AI is highly structured, with a 0,0 transition at 428 nm and peaks at 442, 458, 474, and 489 nm. The deuterated and undeuterated 7AI species exhibit phosphorescence lifetimes of 2.85 and 2.69 s, respectively. The corresponding excitation spectra for their phosphorescence can be ascribed neither to the dimeric species ($S_0^H(D)$) prevailing at 77 K nor to traces of the monomer. Instead, one can in principle assign them to oligomeric species of the compounds or to dimers without symmetrical base-pairing, which precludes double-proton transfer.

The phosphorescence emissions observed here are rather different from those detected by Bulska and Chodkowska,²⁰ possibly because of the higher concentration (10^{-2} M) they used. As can be inferred from the spectrum of Figure 4A, the

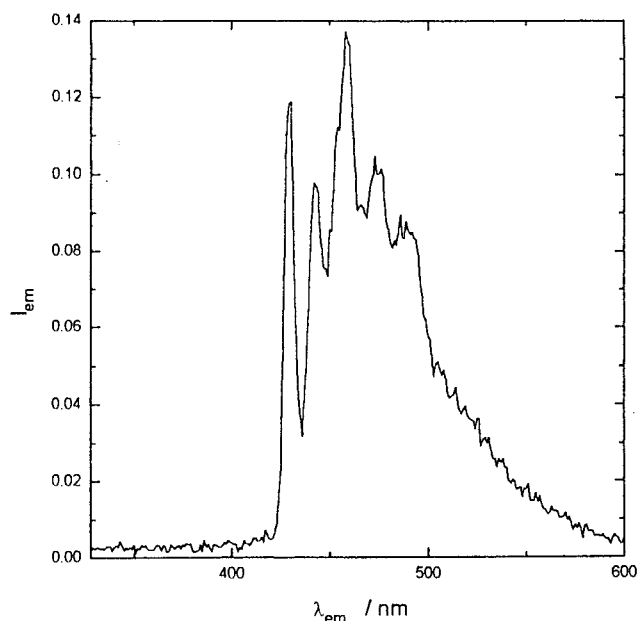
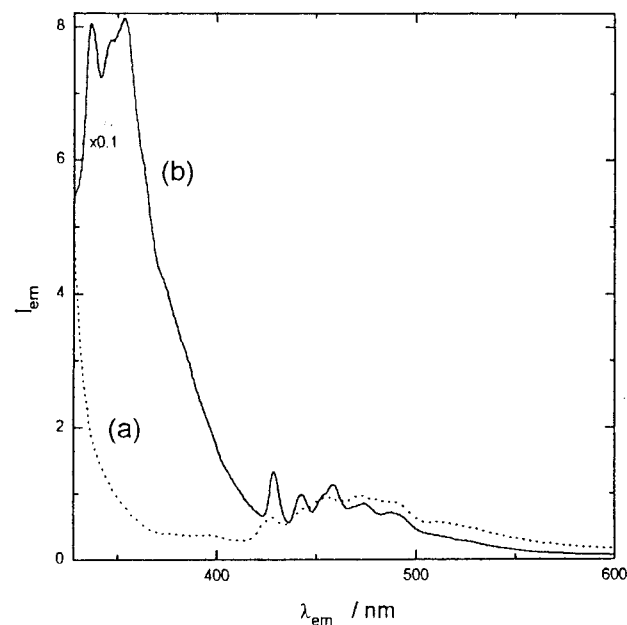


Figure 4. (4A, top) Luminescence spectra for 10^{-4} M solution of 7-azaindole in 2MB at 77 K: (a) undeuterated 7-azaindole and (b) monodeuterated (90%) 7-azaindole ($\lambda_{\text{exc}} = 315$ nm). (B, bottom) Phosphorescence spectra obtained with a delay of 250 μs of monodeuterated 7-azaindole in 2MB at 77 K ($\lambda_{\text{exc}} = 315$ nm).

phosphorescence in the band centered at 475 nm cannot be the dominant component (the PT-fluorescence, F_2 , also being included, cf. Figure 2A). The phosphorescence of the deuterated form, which is better defined (Figure 4A,B), cannot be the dominant emission, as it accounts for less than 30% of the overall emission (Figure 5A).

As shown in Figure 5B, the structured peaks in the 127 K green luminescence (F_2) emission, which is shown to decay completely in less than 250 μs , correspond well with the structured peaks of the long-lived phosphorescence, Figure 4A,B. This observation confirms the earlier observation of El-Bayoumi et al.^{17,18} This apparent spectroscopic contradiction must be investigated further.

Ground-State Proton-Transfer Potential Energy Curves.

On the question of tautomerization of 7AI dimer by double proton transfer from the pyrrole to the opposite pyridine nitrogen

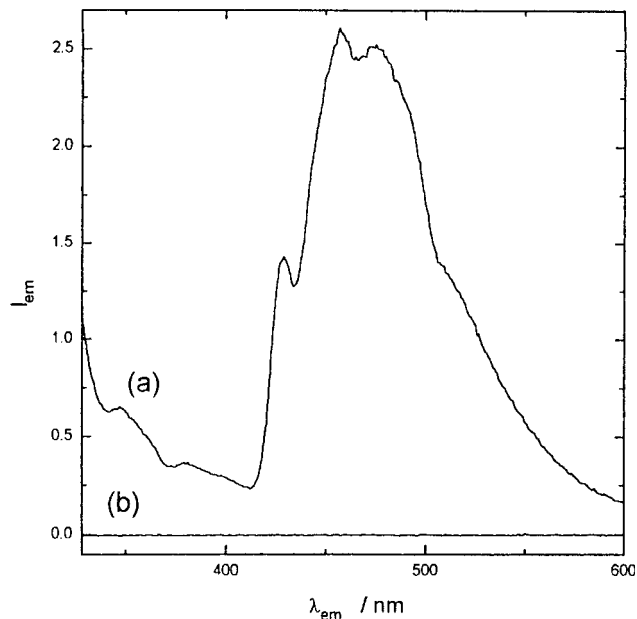
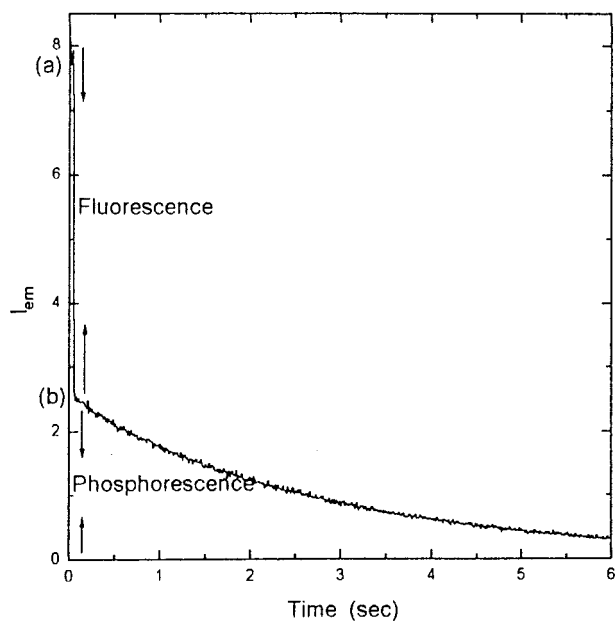


Figure 5. (5A, top) Behavior of the emission intensity of 10^{-4} M solution of deuterated (90%) 7-azaindole in 2MB at 77 K: (a) under steady-state excitation fluorescence + phosphorescence) and (b) after closing the excitation shutter (phosphorescence) ($\lambda_{\text{exc}} = 315$ nm). (B, bottom) Emission spectra for 10^{-4} M solution of 7-azaindole in 2MB at 127 K: (a) without delay and (b) with a delay of 250 μs ($\lambda_{\text{exc}} = 315$ nm).

atom in the dimer (linked via two hydrogen bonds) (scheme A), the first question to be answered is whether the PT-tautomer dimer is stable in the ground-state $S_0^l(D)$, i.e., whether its structure corresponds to a minimum in the proton-transfer potential curve. We find the ground state PT-tautomer dimer is theoretically stable, as the calculated optimized structure for this dimer has all-positive vibrational frequencies in the calculation.

Figure 6 shows the calculated ground state potential energy curves for the double-proton transfer of 7AI at the B3LYP/6-31G** level (DFT), obtained by using optimized molecular structures for both the synchronous and the asynchronous transfer of the protons along the existing hydrogen bonds. As can be seen, the barrier to be overcome by the molecular

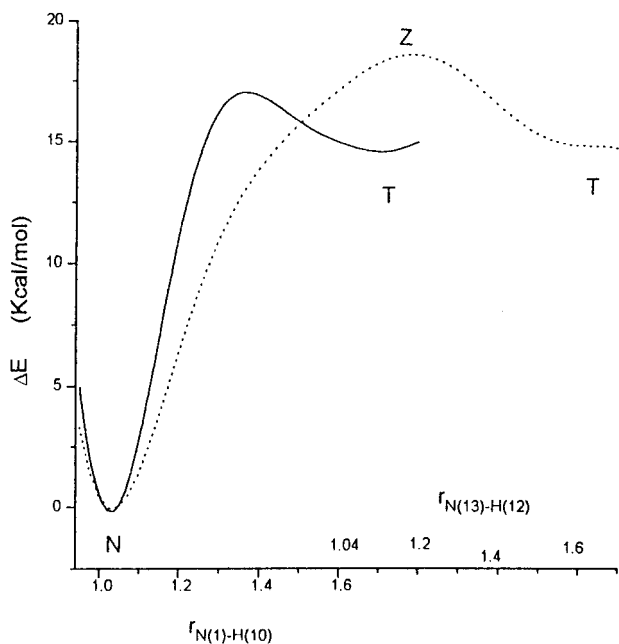


Figure 6. Density functional theory calculated potential energy curves for double proton transfer in ground electronic state of 7-azaindole dimer: (a) synchronous process (—) and (b) asynchronous process (···).

structure of 7AI dimer is lower in the synchronous double transfer than in the asynchronous one, as is also the case in state $S_1^n(D) \rightarrow S_1^t(D)$.^{39,40} It is also worth noting that the energy of such a barrier, 17 kcal/mol, is significantly lower than the 29.48 kcal/mol obtained by Douhal et al.⁴¹ The explanation lies in the fact that the computations of those authors excluded the effect of electron correlation, so they provided no accurate description for the hydrogen bonds or the proton transfers along them.^{36,37}

The presence of a second minimum (Figure 6) suggests that this species may have a long enough lifetime to be trapped transiently as this PT-tautomer is generated via rapid pulsed excitation to the excited state of the normal-tautomer dimer. The Introduction reviews those conflicting reports on the actual metastability of the ground state of the proton-transfer tautomer in the 7AI dimer $S_0^t(D)$, relative to back proton-transfer in the normal tautomer ground-state $S_0^n(D)$. The spectroscopic state must be a short-lived transient. However, in our laboratory we have observed a comparatively long-lived tautomer intermediate, observed by a novel technique. We are currently exploring the origin and nature of this intermediate, which could play a role in DNA transmutation as a longer lived (minutes) chemical intermediate arising from the very short-lived spectroscopic transient.

The potential curve for the $S_0^n(D) \rightarrow S_0^t(D)$ state has a bearing on the PT-tautomer dimer fluorescence. If the region of the potential energy surface for the ground electronic state of the PT-tautomer species contains no minimum, it will represent a repulsive situation that will preclude structuring in the F_2 emission for the PT-tautomer; otherwise, the emission may be structured. As can be seen from the spectra for the F_2 emission in Figure 2A, structuring increases as the temperature is lowered, with peaks at 420, 460, and 480 nm; however, the fact that these peaks coincide with the phosphorescence of 7AI reported by Bulska and Chodkowska²⁰ and their assertion that structuring in this emission is parallel to the presence of the long-lifetime component (phosphorescence), would seem to rule out assignment of the vibronic structuring to the fluorescence. However, as can be seen from Figure 5B, spectrally structured F_2 emission

(of the undeuterated 10% component) of the 7AI at 127 K disappears if detection is delayed by 250 μ s. We can therefore conclude that structuring is inherent in the fluorescence emission of the compound, which confirms the presence of a minimum in the ground electronic state of the dimeric PT-tautomer of 7AI.

Recent discussion of the biprotonic phototautomerism of 7AI dimer has brought a proposal of a two-step mechanism for the photoreaction.^{32,40,42} Our laboratories have reaffirmed the case for a concerted one-step mechanism in three stages: (a) the electronic excitation and charge-density concerted driving force at both H-bonding sites,³⁹ (b) the relation of the conjectured intermediate anion/cation pair which would be present in the intermediate to the electronic states of the anion and cation,⁴⁰ and (c) the energetics of the intermediate cationic potential which an intermediate would require.⁴³

Quantum mechanical (QM) requirements dictate that a molecular dimer should exhibit collective excitation modes. The collective excitation of 7AI dimer pairs was treated as a molecular exciton^{44,45} case in the original paper¹⁶ on 7AI dimer, and recent high-resolution spectroscopy results have confirmed this.^{22,23} Thus, a description of the 7AI dimer electronic excitation as a stepwise process in which each molecule of the H-bonded dimer is successively excited violates the fundamental symmetry requirement (QM. theorem of simultaneous eigenfunctions with commuting operators). In addition, the electromagnetic wave perturbation subjects both molecules of the dimer to the same perturbation. This influence, verified by simultaneous centro-symmetric charge redistribution³⁹ in the excited state, also implies simultaneity of the two proton transfer between H-bonded pyrido-pyrrolo N atom. On the other hand, the triplet state exciton coupling is very weak, leading to the result that the 7AI dimer triplet states (for either tautomer) would be very close to the corresponding 7AI monomer triplet states.

Theoretical calculations including molecular geometries, rotational constants, dipole moments, molecular orbitals and vibrational frequencies for the normal-tautomer and PT-tautomer species of 7AI, together with the calculated thermochemical molecular data corresponding to the normal-tautomer ($S_0^n(D)$) and PT-tautomer ($S_0^t(D)$) dimer will be provided and discussed elsewhere.

Conclusions

The tautomerization of H-bonded 7-azaindole (7AI) base pairs and its spectroscopic consequences have been delineated in a comprehensive photophysical investigation. Particular attention was focused on the mechanism of the biprotonic transfer, and the properties of the normal-tautomer dimer vs the proton-transfer tautomer dimer.

The dimerization of 7AI and its temperature dependence are accurately defined by experimental absorption and fluorescence excitation spectra. It is shown that below 227 K in 10^{-4} M solution in 2-methylbutane (2MB) the 7AI exists exclusively as its double-H-bonded dimer. At 298 K in 10^{-6} M solutions in 2MB the absorption spectrum indicates the unique presence of the 7AI monomer.

For the double-H-bonded dimer formed by the undeuterated 7-AI, only the proton-transfer-tautomer fluorescence ($S_1^t(D) \rightarrow S_0^t(D)$) is observed (10^{-4} M solution in 2-MB below 227 K), the normal-tautomer dimer ($S_1^n(D)$) being essentially non-emitting.

For the double-H-bonded dimer formed by mono-deuterated 7AI species (at the N-H pyrrolic site), only normal-tautomer fluorescence ($S_1^n(D) \rightarrow S_0^n(D)$) is observed (10^{-4} M solution in

2-MB below 227 K), the biprotonic transfer being restricted essentially by the deuteration. A partial deuteration yields an illusory dual fluorescence, as seen for the mixture.

The observations of the effect of deuteration on the biprotonic transfer in H-bonded 7AI dimers demonstrate that the molecular tautomerization mechanism involves quantum mechanical tunneling through the excited-state potential barrier.

The phosphorescence (0,0 band) at 430 nm previously reported for 7AI in dilute solutions (10^{-5} M) in hydrocarbon glass solvent at 77 K is obviously the monomer $T_1 \rightarrow S_0$ emission. This phosphorescence is observed strongly in the deuterated 7AI dimer spectrum exhibiting a very detailed vibrational structure, with 0,0 at 430 nm, and a half-life ~ 3 s. The observation of the same structural peaks appearing in the proton-transfer dimer fluorescence ($S_1^1(D) \rightarrow S_0^1(D)$) as observed by previous researchers, is confirmed. This coincidence remains as a puzzle for future research.

Theoretical calculations on the ground state proton-transfer potential energy curves obtained in the Density Functional Theory framework (B3LYP/6-31G**) are shown to conform accurately to the observed experimental results.

Acknowledgment. We are pleased to acknowledge the critical suggestions made by Huaping Li in our Florida Laboratory. We are also greatly indebted to Dirección General de Investigación Científico y Técnica (Spain) for the support project PB98-063.

References and Notes

- (1) Watson, J. D.; Crick, F. H. C. *Nature* **1953**, *171*, 737–738, 964–967.
- (2) Drake, J. W. *The Molecular Basis of Mutation*; Holden-Day: San Francisco, 1970.
- (3) Auerbach, C. *Mutations Research. Problems, Results and Perspectives*; Chapman and Hall: London, 1976.
- (4) Löwdin, P. O. *Adv. Quantum Chem.* **1965**, *2*, 213–360 and references therein.
- (5) Lawley, P. D.; Brookes, P. *Nature* **1961**, *192*, 1081; *J. Mol. Biol.* **1962**, *4*, 216.
- (6) Rosen, P. *Int. J. Quantum Chem.* **1975**, *9*, 473.
- (7) Cooper, W. G. *Int. J. Quantum Chem.* **1978**, *14*, 71–89; *Int. J. Quantum Chem. Quantum Biol. Symp.* **1978**, *5*, 463–467.
- (8) Sevilla, M. D.; Becker, D.; Yan, M.; Summerfield, S. R. *J. Phys. Chem.* **1991**, *95*, 3409–3415.
- (9) Stemp, E. D. A.; Arkin, M. R.; Barton, J. K. *J. Am. Chem. Soc.* **1997**, *119*, 2921–2925.
- (10) Itoh, R. *Prog. Theor. Phys.* 1961 Supp. 17, 69.
- (11) Ladik, J. *J. Theor. Biol.* **1964**, *6*, 201.
- (12) Rein, R.; Harris, F. E. *J. Chem. Phys.* **1964**, *41*, 3393–3401; **1965**, *42*, 2177–2180; **1965**, *43*, 4415–4421.
- (13) Eisinger, J. *Photochem. Photobiol.* **1968**, *7*, 597–612.
- (14) Lamola, A. *Photochem. Photobiol.* **1968**, *7*, 619–632.
- (15) Kasha, M.; Horowitz, P.; El-Bayoumi, M. A. In *Molecular Spectroscopy, Modern Research*; Rao, K. N., Mathews, C. W., Eds.; Academic Press: 1972; Chapter 6.
- (16) Taylor, C. A.; El-Bayoumi, M. A.; Kasha, M. *Proc. Acad. Natl. Sci. U.S.A.* **1969**, *63*, 253–260.
- (17) Ingham, K. C.; Abu-Elgheit, M.; El-Bayoumi, M. A. *J. Am. Chem. Soc.* **1971**, *93*, 5023–5025.
- (18) Ingham, K. C.; El-Bayoumi, M. A. *J. Am. Chem. Soc.* **1974**, *96*, 1674–1682.
- (19) El-Bayoumi, M. A.; Avouris, P.; Ware, W. R. *J. Chem. Phys.* **1975**, *62*, 2499–2500.
- (20) Bulska, H.; Chodkowska, A. *J. Am. Chem. Soc.* **1989**, *102*, 3259.
- (21) Hetherington, III, W. M.; Michels, R. H.; Eisenthal, K. B. *Chem. Phys. Lett.* **1979**, *66*, 230–233.
- (22) Fuke, K.; Yoshiuchi, H.; Kaya, K. *J. Phys. Chem.* **1984**, *88*, 5840–5844.
- (23) Fuke, F.; Kaya, K. *J. Phys. Chem.* **1989**, *93*, 614–621.
- (24) Waluk, J.; Bulska, H.; Pakula, B.; Sepiol, J. *J. Lumin.* **1981**, *24/25*, 519–522.
- (25) Bulska, H.; Grabowska, A.; Pakula, B.; Sepiol, J.; Waluk, J.; Wild, U. P. *J. Lumin.* **1984**, *29*, 65–81.
- (26) Tokumura, K.; Watanabe, Y.; Itoh, M. *Chem. Phys. Lett.* **1984**, *111*, 379–382.
- (27) Tokumura, K.; Watanabe, Y.; Itoh, M. *J. Phys. Chem.* **1986**, *90*, 2362–2366.
- (28) Tokumura, K.; Watanabe, Y.; Udagawa, M.; Itoh, M. *J. Am. Chem. Soc.* **1987**, *109*, 1346–1350.
- (29) Share, P.; Pereira, M.; Sarisky, M.; Repinec, S.; Hochstrasser, R. M. *J. Lumin.* **1991**, *48/49*, 204–208.
- (30) Suzuki, T.; Okuyama, U.; Ichimura, T. *J. Phys. Chem. A* **1997**, *101*, 7047–7052.
- (31) Chou, P. T.; Yu, W. S.; Chen, Y. C.; Wei, C. Y.; Martinez, S. S. *J. Am. Chem. Soc.* **1998**, *120*, 12927–12934.
- (32) Chachisvilis, M.; Fiebig, T.; Douhal, A.; Zewail, A. H. *J. Phys. Chem. A* **1998**, *102*, 669–673.
- (33) Frisch, M. J.; Trucks, G. W.; Schlegel, H. B.; Gill, P. M. W.; Johnson, B. G.; Robb, M. A.; Cheeseman, R.; Keith, T.; Petersson, G. A.; Montgomery, J. A.; Raghavachari, K.; Al-Laham, M. A.; Zakrzewski, V. G.; Ortiz, J. V.; Foresman, J. B.; Peng, C. Y.; Ayala, P. Y.; Chen, W.; Wong, M. W.; Andres, J. L.; Replogle, E. S.; Gomperts, R.; Martin, R. L.; Fox, D. J.; Binkley, J. S.; Defrees, D. J.; Baker, J.; Stewart, J. P.; Head-Gordon, M.; Gonzalez, C.; Pople, J. A. *Gaussian 94*, revision B.2; Gaussian, Inc.: Pittsburgh, PA, 1995.
- (34) Hariharan, P. C.; Pople, J. A. *Chem. Phys. Lett.* **1972**, *16*, 217–219.
- (35) Becke, A. D. *J. Chem. Phys.* **1993**, *98*, 5648–5652.
- (36) Catalán, J.; Palomar, J.; de Paz, J. L. G. *Chem. Phys. Lett.* **1997**, *269*, 151–155.
- (37) Catalán, J.; Palomar, J.; de Paz, J. L. G. *J. Phys. Chem. A* **1997**, *101*, 7914–7921.
- (38) Mulliken, R. S.; Rieke, C. A. *Phys. Soc. London, Rep. Prog. Phys.* **1941**, *8*, 231–273.
- (39) Catalán, J.; del Valle, J. C.; Kasha, M. *Proc. Acad. Natl. Sci. U.S.A.* **1999**, *96*, 8338–8943. **1999**, *96*, 8338–8943.
- (40) del Valle, J. C.; Kasha, M.; Catalán, J. *Int. J. Quantum Chem.* **2000**, *77*, 118–127.
- (41) Douhal, A.; Guallar, V.; Moreno, M.; Lluch, J. M. *Chem. Phys. Lett.* **256**, 370–376.
- (42) Former, D. E.; Poth, L.; Wisniewski, E. S.; Castleman, A. W., Jr. *Chem. Phys. Lett.* **1998**, *287*, 1–7.
- (43) Catalán, J.; del Valle, J. C.; Kasha, M. *Chem. Phys. Lett.* **2000**, *318*, 629–636.
- (44) McRae, E. G.; Kasha, M. The Molecular Exciton Model. In *Physical Processes in Radiation Biology*; Augenstein, Rosenberg, Mason, Eds.; Academic Press: New York, 1964; pp 23–42.
- (45) Kasha, M. Molecular Excitons in Small Aggregates. In *Spectroscopy of the Excited State*; DiBartolo, B., Ed.; Plenum Press: New York, 1976; pp 337–363.